

Highly Regioselective Solid-State Photodimerization of Naphthoquinolizinium Salts

Heiko Ihmels,^{*,[a]} Christian J. Mohrschlatt,^[a] Andreas Schmitt,^[a] Milena Bressanini,^{[a],[‡]} Dirk Leusser,^[b] and Dietmar Stalke^[b]

Dedicated to Professor Manfred Christl on the occasion of his 60th birthday

Keywords: Cycloadditions / Heterocycles / π interactions / Photochemistry / Solid-state reactions

The photodimerization of benzo-annellated acridizinium derivatives, namely naphtho[1,2-*b*]quinolizinium and naphtho[2,1-*b*]quinolizinium bromide, has been investigated in solution and in the solid state. Irradiation of the naphthoquinolizinium salts in solution gave all possible regioisomers in an unselective [4+4] photocycloaddition reaction. In contrast, the irradiation of crystalline samples resulted in regioselective dimerization to give the *anti*-head-to-tail photodimers.

The reactivity in the crystalline phase depended significantly on the solvent used for crystallization. The results are discussed on the basis of X-ray diffraction analyses that showed that the selectivity of the photodimerization in the solid state was the result of *anti*-head-to-tail preorganization of pairs of molecules in the crystalline state.

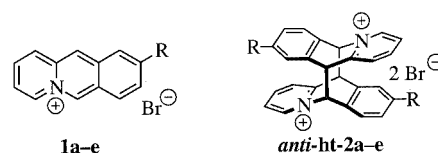
(© Wiley-VCH Verlag GmbH, 69451 Weinheim, Germany, 2002)

Introduction

Solid-state organic photoreactions have become a useful tool in synthetic organic chemistry, since there is a remarkable number of highly selective transformations that occur on irradiation in the crystalline medium.^[1–5] Among the reactions that have been investigated in the solid state, the [4+4] photocycloaddition^[6,7] offers great potential in organic synthesis.^[8–10] In this context, acridizinium derivatives^[11] may be used to study this reaction in the solid state, because they – like anthracenes^[12,13] – dimerize on irradiation in a clean [4+4] photocycloaddition reaction.^[14–17]

In particular, the fact that photoreactions of acridizinium salts can yield four different regioisomeric dimers allows the regioselectivity of the photodimerization in the solid state to be investigated. Thus, irradiation of *single crystals* of the parent acridizinium **1a**^[14,16] and of 9-methyl- (**1b**)^[15] and 9-chloroacridizinium (**1c**)^[18] exclusively gave the corresponding *anti*-head-to-tail dimers **anti-ht-2a–c** in a topochemical reaction. In the cases of the salts **1a** and **1c** in the *polycrystalline state*, in contrast, irradiation yielded all four possible

regioisomers of the photodimers.^[17,18] Nevertheless, it has been demonstrated that the introduction of moderate π -donor substituents, namely methoxy and bromo functionalities, at the 9-positions of the acridizinium salts **1d** and **1e** allows the regioselective solid-state photodimerization to be performed to give the *anti*-head-to-tail dimers **anti-ht-2d** and **anti-ht-2e** exclusively either in the single crystal or in the polycrystalline state.^[17] This regioselectivity still persisted at full conversion and was explained in terms of strong directional π stacking of two molecules in the solid state. Such directional effects^[20,21] have previously been observed in photodimerizations of alkenes,^[22,23] and are proposed to be the result of the introduction of a distinct dipole moment into the molecules, forcing the molecules to arrange in an antiparallel manner.



a: R = H; b: R = Me; c: R = Cl; d: R = Br; e: R = OMe

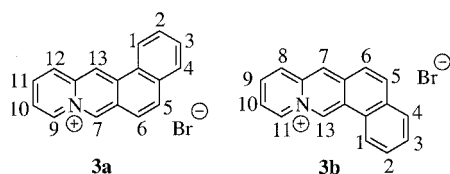
^[a] Institute of Organic Chemistry, University of Würzburg, Am Hubland, 97074 Würzburg, Germany
Fax: (internat.) + 49-(0)931/888-4606
E-mail: ihmels@chemie.uni-wuerzburg.de

^[b] Institute of Inorganic Chemistry, University of Würzburg, Am Hubland, 97074 Würzburg, Germany

^[‡] Visiting scientist from: Department of Pharmaceutical Sciences, University of Padova, 35131 Padova, Italy

In our investigations of substituent effects on the solid-state photoreactions of acridizinium derivatives we have now focused our intention on the influence of an extension of the aromatic system on the π stacking, which may further affect the solid-state reactivity. The solid-state photochemistry of the representative benzo-annellated acridizinium

derivative, namely naphthoquinolizinium bromides **3a** and **3b**, has therefore been investigated and is presented here.



Results

Absorption and Emission Properties

The known naphthoquinolizinium bromides **3a** and **3b** were synthesized according to literature procedures.^[24] They are yellow solids, and their solutions each exhibit a resolved absorption band for the long-wavelength S_0-S_1 transition in the UV/Vis region (Table 1), along with the more intense S_0-S_2 and S_0-S_3 transitions at shorter wavelengths. The UV absorption bands have zero onsets at $\lambda \approx 425$ nm (**3a**) and $\lambda \approx 410$ nm (**3b**). Each compound exhibits a broad fluorescence band on excitation, with moderate fluorescence quantum yields (Table 1). The absorption and the emission properties of the naphthoquinolizinium salts **3a** and **3b** are only slightly solvent-dependent. The absorption and emission spectra of **3a** in methanol are presented in Figure 1.

Table 1. Absorption and emission data of naphthoquinolizinium bromides **3a** and **3b** in solution

Solvent	3a				3b			
	λ_{abs} [a] [nm]	log ϵ	λ_{em} [b] [nm]	ϕ_{em} [c]	λ_{abs} [a] [nm]	log ϵ	λ_{em} [b] [nm]	ϕ_{em} [c]
Buffer ^[d]	402	3.84	418	0.13	391	4.34	422	0.26
H ₂ O	402	3.80	419	0.16	392	4.31	422	0.32
MeOH	403	3.90	420	0.18	393	4.33	422	0.48
CH ₃ CN	402	3.87	420	0.20	392	4.36	421	0.39
DMSO	404	3.99	— ^[e]	— ^[e]	395	4.40	— ^[e]	— ^[e]

[a] $c = 10^{-4}$ M, S_0-S_1 transition, maximum at longest wavelength. [b] $\lambda_{\text{ex}}(\mathbf{3a}) = 380$ nm; $\lambda_{\text{ex}}(\mathbf{3b}) = 370$ nm; $c = 10^{-5}$ M. [c] Relative to quinine sulfate in 1 N H₂SO₄; error: ± 0.02 . [d] 10 mM phosphate buffer (pH = 7.0). [e] Not determined.

Both quinolizinium salts **3a** and **3b** emit in the solid state. The solid-state fluorescence spectrum of **3a**, crystallized from ethanol, for example, exhibits several broad emission bands between $\lambda = 400$ and 600 nm (Figure 2). The solid-state excitation spectrum of **3a** showed a broad band in the same UV/Vis region in which **3b** absorbed in solution ($\lambda \approx 340-420$ nm).

Photoreactions in Solution

Irradiation of the quinolizinium bromides **3a** and **3b** at $\lambda > 395$ nm (Heraeus TQ 150, high-pressure Hg lamp) in

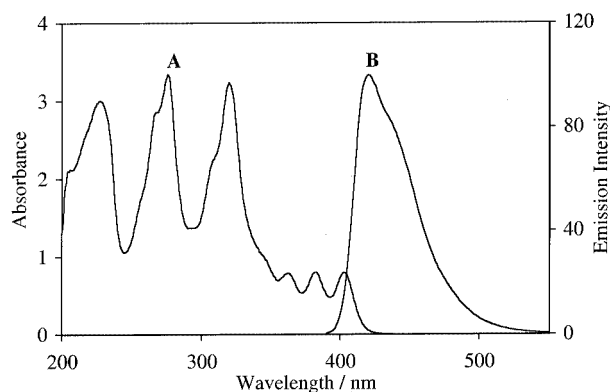


Figure 1. Absorption (A) and emission spectra (B) of **3a** in methanol solution [A: $c(\mathbf{3a}) = 10^{-4}$ M; B: $c(\mathbf{3a}) = 10^{-5}$ M; $\lambda_{\text{ex}} = 380$ nm, emission intensity scale is in arbitrary units]

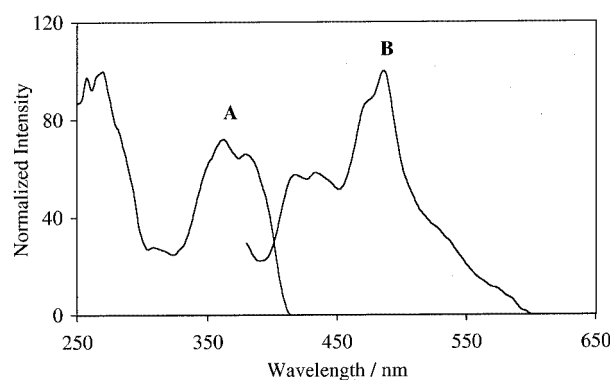


Figure 2. Solid-state fluorescence excitation (A) and emission spectra (B) of **3a** (A: $\lambda_{\text{em}} = 440$ nm; B: $\lambda_{\text{ex}} = 380$ nm)

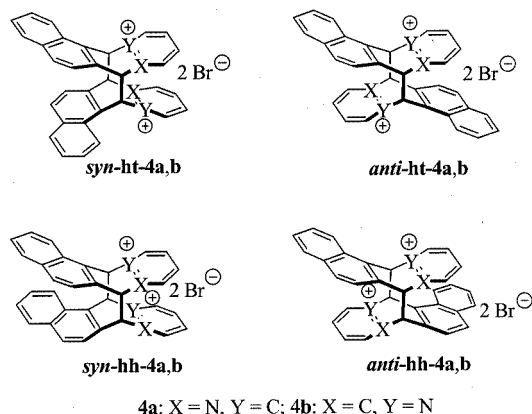
methanol solutions resulted in all four regioisomers **4a** and **4b**. The progress of the photoreactions was monitored by ¹H NMR spectroscopic analysis of the reaction mixtures, as the formation of the photodimers **4** was indicated by the appearance of the characteristic NMR signals of the bridgehead protons. The mixtures of the photoproducts of **3a** and **3b** could not be separated by the usual chromatographic methods. Interestingly, the photoreactions could not be carried out to complete conversion. For example, after 4 h of irradiation of **3b**, a degree of conversion of 58% was observed (Table 2, Entry 10), and this level of conversion had not changed (within the error limits) after an additional 2 h irradiation (Table 2, Entries 11 and 12). Similarly, a degree of conversion of 49% (Table 2, Entry 1) was observed after irradiation of **3a** for 3 h, and this also did not increase on prolonged irradiation.

In the case of derivative **3a**, the substantial degree of overlap of the bridgehead proton signals with the aromatic signals of the photodimers prevented the determination of the product ratio by ¹H NMR spectroscopy. However, the ratio of head-to-tail (ht) to head-to-head (hh) dimers of naphthoquinolizinium **3b** could be determined directly from the reaction mixture by ¹H NMR spectroscopic analysis (Table 2). Thus, irradiation of the derivative **3b** at

Table 2. Results of the irradiation ($\lambda \geq 395$ nm, 20 °C) of the naphthoquinolinizinium bromides **3a** and **3b** in different media

Entry	Compd.	Medium	Time ^[a] [h]	Conv. ^[a] [%]	M.B. ^[a] ^[b] [%]	ht/hh ^[a] ^[c]
1	3a	[D ₄]MeOH	3	49	>95	— ^[d]
2	3a(MeOH)	crystal ^[e]	24	37	>95	>95 ^[f] ; < 5
3	3a(MeOH)	crystal ^[e]	47	35	>95	>95 ^[f] ; < 5
4	3a(EtOH)	crystal ^[g]	24	74	>95	>95 ^[f] ; < 5
5	3a(EtOH)	crystal ^[g]	72	81	>95	>95 ^[f] ; < 5
6	3b	[D ₄]MeOH	0.5	17	>95	50:50
7	3b	[D ₄]MeOH	1	33	>95	50:50
8	3b	[D ₄]MeOH	2	42	>95	50:50
9	3b	[D ₄]MeOH	3	50	>95	57:43
10	3b	[D ₄]MeOH	4	58	>95	50:50
11	3b	[D ₄]MeOH	5	56	>95	57:43
12	3b	[D ₄]MeOH	6	60	>95	55:45
13	3b(EtOH)	crystal ^[g]	168	38	>95	>95 ^[f] ; < 5
14	3b(AcOH)	crystal ^[h]	240	28	>95	>95 ^[f] ; < 5
15	3b(H₂O)	crystal ^[i]	240	<5	>95	—
16	3b(PrOH)	crystal ^[j]	240	<5	>95	—
17	3b(MeOH)	crystal ^[e]	48	90	>95	>95 ^[f] ; < 5

[a] Determined by ¹H NMR spectroscopic analysis, relative to hexamethyldisiloxane as internal standard, estimated error: $\pm 5\%$. [b] M.B. = Mass balance. [c] hh = head-to-head photodimers; ht = head-to-tail photodimers. [d] Could not be determined. [e] From methanol. [f] Only *anti* isomer detected. [g] From ethanol. [h] From acetic acid. [i] From water. [j] From methanol/2-propanol.



$\lambda > 395$ nm resulted in the formation of head-to-head and head-to-tail dimers in a ratio of approximately 1:1 (Table 2).

The hh and ht dimers were distinguished by the signal multiplicities of the protons at C-7 and C-13. The bridge-head protons of the two head-to-tail dimers *syn-ht-4* and *anti-ht-4* display two doublets with characteristic coupling constants of $J \approx 11$ Hz, whereas these protons in the head-to-head dimers *syn-hh-4* and *anti-hh-4* give singlets in their ¹H NMR spectra. Thus, the ht/hh ratio in the **3b** photoproduct mixture was evaluated by determination of the integrals of the corresponding proton signals (Table 2). The ratio of the *anti* and *syn* dimers could not be determined, due to the overlap of the relevant signals, which prevented the ROESY NMR experiments required for the assignment of the *syn* and *anti* structures.

Since full conversion of **3a** and **3b** was not achieved under the conditions employed, the photoreactivities of the

photodimers *anti-ht-4a* and *anti-ht-4b* were also investigated. Thus, samples of the dimers *anti-ht-4a* or *anti-ht-4b* in methanol were irradiated with monochromatic fluorescence-spectrophotometer light ($\lambda = 390$ nm), and the reactions were monitored by UV spectroscopy. The reaction progress in each case was indicated by the increase in the characteristic absorption bands of the respective monomer **3a** or **3b**. It should be noted that the UV spectrum of the starting material revealed in each case that trace amounts of the corresponding monomer were present in solution. An increased irradiation time slowly brought about the formation of the monomers **3a** and **3b**, as shown for the example of the irradiation of *anti-ht-4b* (Figure 3). To ensure that the cycloreversion proceeded without the formation of by-products, the photoreaction of *anti-ht-4b* was also monitored by ¹H NMR spectroscopy, irradiation of *anti-ht-4b* in [D₆]DMSO at $\lambda > 395$ nm exclusively yielding the monomer **3b** (Figure 4). DMSO was used as solvent because of the better solubility of the dimer *anti-ht-4b* in it.

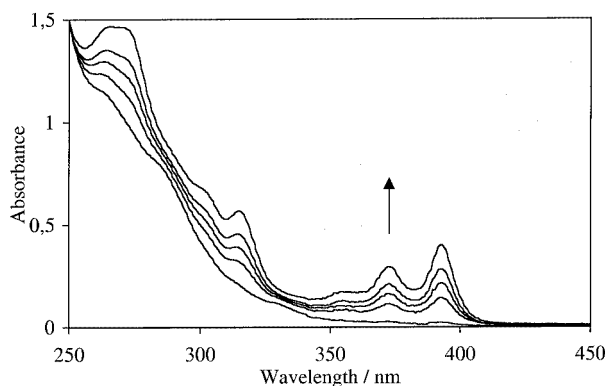


Figure 3. Photoinduced cycloreversion of the dimer *anti-ht-4b* monitored by UV/Vis spectroscopy [$\lambda = 390$ nm, $c(\text{anti-ht-4b}) = 6.0 \cdot 10^{-5}$ M, the arrow indicates the successive increase of the signal intensity on irradiation for 0, 30, 60, 120, 180 min]

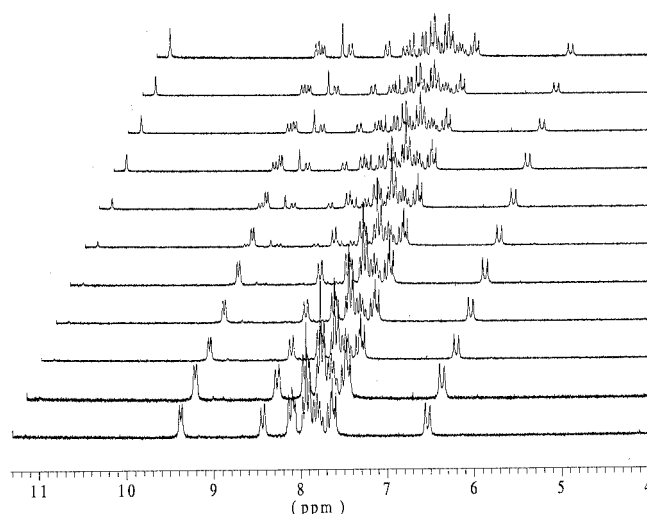
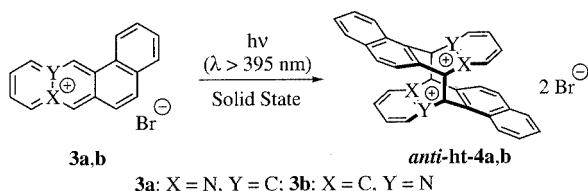


Figure 4. Photoinduced cycloreversion of the dimer *anti-ht-4b* monitored by ¹H NMR spectroscopy [$\lambda > 395$ nm, $c(\text{anti-ht-4b}) = 1.5 \cdot 10^{-2}$ M, spectra are arranged from front to back in order of increasing irradiation time: 0, 0.5, 1.0, 1.5, 2.0, 2.5, 3.0, 3.5, 4.0, 4.5, and 5.0 min]

Photoreactions in the Solid State

The naphthoquinolizinium salts **3a** and **3b** were crystallized from different solvents, and the ground crystalline samples were irradiated at $\lambda > 395$ nm (Heraeus TQ 150, high-pressure Hg lamp) at 10 °C (Table 2). Irradiation of naphthoquinolizinium **3a**(EtOH),^[25] which had been crystallized from ethanol, exclusively afforded the *anti*-head-to-tail dimer *anti*-ht-**4a** (Scheme 1, Table 2, Entries 4 and 5). A maximum degree of conversion of 81% was achieved after 3 d, and the dimer *anti*-ht-**4a** was isolated by recrystallization in 51% yield. On irradiation of solid samples of **3a**(MeOH), which had been crystallized from methanol, the dimer *anti*-ht-**4a** was also formed exclusively, although the level of conversion (37%) could not be improved on even after prolonged irradiation times (Table 2, Entries 2 and 3). In both cases, the regioselectivity remained, even with solid samples not of single-crystal quality. Similarly, irradiation of polycrystalline solid samples of salts **3b**(EtOH) or **3b**(AcOH), crystallized from ethanol or from acetic acid, respectively,



Scheme 1

exclusively provided the dimer *anti*-ht-**4b** (Scheme 1, Table 2, Entries 13 and 14). However, the degrees of conversion were low (38 and 28%) and did not increase even after several days of irradiation. With solid samples of **3b**(MeOH) (i.e., crystallized from methanol, Table 2, Entry 17) the degree of conversion was almost complete, and the dimer was isolated by recrystallization in 58% yield. In contrast, solid samples of **3b** crystallized from water or from methanol/2-propanol were photoinert in the solid state (Table 2, Entries 15 and 16).

The structural assignments of the isolated dimers *anti*-ht-**4a** and *anti*-ht-**4b** were performed by means of one- and two-dimensional NMR experiments, mainly on the basis of chemical shifts and signal patterns of the bridgehead protons in the ¹H NMR spectrum, as already described for the unsubstituted regiomer dimers **2a–e**.^[17,19] The head-to-tail structures were confirmed by the characteristic shifts and multiplicities of the bridgehead protons [*anti*-ht-**4a**: $\delta = 7.17$ (d, $J = 10.7$ Hz, 13-H); *anti*-ht-**4b**: $\delta = 6.53$ (d, $J = 10.9$ Hz, 7-H), numbering according to that shown for the monomers **3a** and **3b**]. The signals of the bridgehead protons α to the nitrogen atom could not be analysed, because of overlap with signals of aromatic protons. The *anti* structures of the isolated dimers were determined by ROESY NMR experiments, in which the characteristic NOE interactions between the proton pairs 1-H/9'-H and 6-H/12'-H in *anti*-ht-**4a** and 1-H/8'-H and 6-H/11'-H in *anti*-ht-**4b** were demonstrated unambiguously.

Discussion

The photodimerization of benzo[*a*]anthracene (the parent hydrocarbon system of **3a** and **3b**) and the structural assignment of its photodimers have been reported,^[26–28] but no studies of the regioselectivity of the photoreaction and of the solid-state photoreactivity have been presented. Like benzo[*a*]anthracene, the naphthoquinolizinium salts **3a** and **3b** yielded the analogous photoproducts **4** on irradiation. Moreover, the photoreactivities of the naphthoquinolizinium salts **3a** and **3b** in methanol solution resembled that observed for the parent acridizinium **2a**.^[29] Thus, the introduction of another benzene ring onto an acridizinium chromophore and the introduction of a quaternary bridgehead nitrogen atom into the benzo[*a*]anthracene structure had not significantly distorted the electronic structure of the anthracene chromophore, and so comparable photochemical properties were observed for these compounds.

Photoreactions in Solution

Interestingly, the photodimerization reaction of salts **3a** and **3b**, unlike that of the acridizinium **1**, could not be performed with full conversion, a steady ratio between the starting material and the products being attained in each case. Since photodimerization of aromatic compounds is a reversible reaction (i.e., thermal or photoinduced cycloreversion to the monomers is possible),^[12] photostationary equilibria may be assumed under these conditions i.e., photodimerization and photoinduced cycloreversion taking place to the same extents. Figure 5 (spectrum **B**) presents the absorption spectrum of the mixture of **3b** and **4b** in their photostationary state. We observed that the composition of the photolysate of **3a** and **3b** did not change at room temperature in the dark even after several days or upon warming to 40 °C for 90 h (monitored by ¹H NMR spectroscopy in [D₆]DMSO), so the observed cycloreversion is likely to be *photoinduced*. This assumption was confirmed by the successful reversion of the photodimers on irradiation at $\lambda > 395$ nm (Figures 3 and 4). However, the UV spectra of the dimers *anti*-ht-**4a** and *anti*-ht-**4b** showed that these compounds did not absorb at $\lambda > 350$ nm (Figure 5, spectrum **A**, note small traces of the monomer). Thus, with the filter used ($\lambda > 395$ nm), *direct* photoinduced cycloreversion could not have taken place. In addition, we observed that the photoinduced cycloreversion also took place when small amounts (0.1 mol-equiv.) of monomer were added to a solution of the dimer (see Exp. Sect.). From these observations we have tentatively concluded that the cycloreversion may be sensitized by electron transfer from the monomer molecules. Thus, a naphthoquinolizinium molecule **3** in its excited state and the photodimer **4** could be involved in an electron-transfer reaction to give the radical **3-red** and the radical cation of the dimer **4-ox**. In Scheme 2 this reaction is shown for the example of **3a** and *anti*-ht-**4a**. The oxidized photodimers **4-ox** should quickly revert to the monomers, as has been described for radical cations of anthracene photodimers, formed similarly by photoinduced

electron transfer with dicyanoanthracene or chloranil.^[30–32] The fact that this reaction also took place with authentic samples of photodimers would have been due to unavoidable traces of monomer in solution. To estimate the energetics of the electron transfer, we calculated the free energy (ΔG_{PET}) of the photoinduced electron transfer between an excited acridizinium **1a** ($E_{\text{red}}^* \approx 2.4 \text{ V}^{[33]}$) and naphthalene ($E_{\text{ox}} = 2.08 \text{ V}$) as a model reaction. According to the Rehm–Weller equation the free energy of this reaction should be approximately $\Delta G_{\text{PET}} \approx -7.4 \text{ kcal/mol}$ (i.e., the reaction should be slightly exergonic). Since the two systems are roughly comparable, we concluded that photoinduced electron transfer between **3a** and **3b** and their respective photodimers **4a** and **4b** might also be thermodynamically favourable. Further evidence for this mechanism was provided by the independent formation of radical cations of the dimer *anti*-ht-**4b** on treatment with tris(bromophenyl)aminium hexafluoroantimonate; the addition of this one-electron oxidant to *anti*-ht-**4b** in DMF was monitored by UV spectroscopy, and the formation of the naphthoquinolizinium salt **3b** was indicated by the appearance of the characteristic absorption band of **3b** at $\lambda = 393 \text{ nm}$.

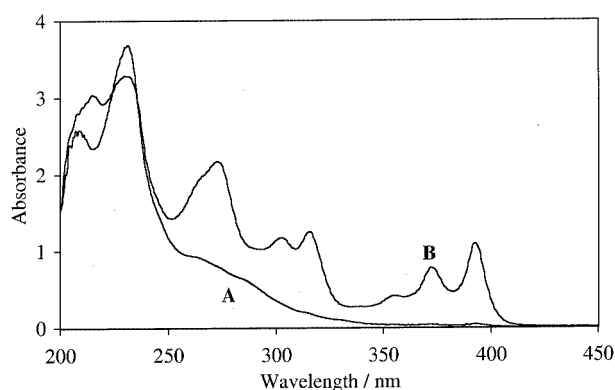
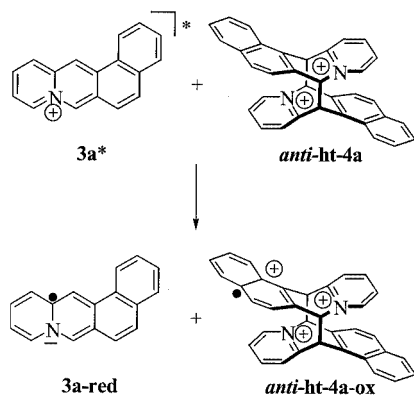


Figure 5. Absorption spectra of the photodimer *anti*-ht-**4b** (A); $c = 10^{-4} \text{ M}$, and of the photostationary state after 6 h of irradiation of **3b** at $\lambda > 395 \text{ nm}$ (B); conversion: 58%; $c(\mathbf{3b} + 2 \times \mathbf{4b}) = 10^{-4} \text{ M}$



Scheme 2

Photoreactions in the Solid State

The solid-state photodimerizations of the different solid forms of **3a** and **3b** obtained by crystallization from different solvents proceeded with a high regioselectivity that could not be achieved in solution, and so represent new examples of selectivity enhancement of a photoreaction upon changing the reaction medium from solution to the crystalline state. Most notably, even irradiation of polycrystalline samples exclusively gave one photoproduct, in sharp contrast to the behaviour of the parent acridizinium salt **1a**.^[17] In terms of the topochemical behaviour during the solid-state photoreaction of the naphthoquinolizinium derivatives **3a** and **3b**, the regioselectivity of the solid-state dimerization may be explained by the arrangement of the molecules in the crystalline state, which is favourable for an *anti*-head-to-tail dimerization. X-ray diffraction analyses of single crystals obtained from the naphthoquinolizinium salts **3a**(MeOH) and **3a**(EtOH) confirmed these proposed solid-state arrangements of the quinolizinium salts.

Both solid forms, **3a**(EtOH) and **3a**(MeOH), crystallize with lattice solvents. In the crystal lattice of **3a**(EtOH), ethanol molecules are present, whereas in **3a**(MeOH), methanol and water molecules cocrystallize with the quinolizinium bromide. In both cases, the lattice solvents form hydrogen bonds with the bromide ions and are well separated from the quinolizinium molecules. It may therefore reasonably be assumed that the lattice solvents should not interfere directly with the solid-state photoreaction.

In the case of the photoactive salt **3a**(EtOH) (crystallized from ethanol), the crystal lattice consists of pairs of chromophores arranged well for *anti*-head-to-tail dimerization (Figure 6). For a quantitative analysis, the distances d and d' between the opposite carbon atoms (i.e., C7 and C13) potentially involved in new C–C bonds on photodimerization were taken as the crucial structural parameters. The postulated ideal value is $d < 420 \text{ pm}$, as deduced from earlier results of structure-reactivity correlations for the solid-state dimerization of anthracenes and alkenes.^[34]

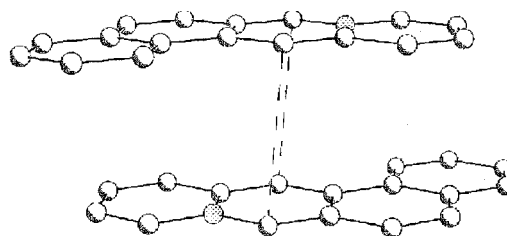


Figure 6. Arrangement of two molecules of **3a**(EtOH), crystallized from ethanol, in the solid state (a pair of the two closest molecules is shown; counter-anions and lattice solvent are omitted for clarity, dotted lines indicate the bonds formed in the course of the photoreaction)

The observed structural features of compound **3a**(EtOH) resemble those of the acridizinium salts **1a–d**.^[14–16,19] Thus, the distances between the reaction centres, C7–C13' and C13'–C7, are suitable for solid-state photodimeriz-

ation ($d = d' = 362$ pm); however, the two molecules are slightly shifted towards each other and exhibit the characteristic “offset” of π -stacked aromatic molecules.^[35] This slight deviation from an ideal overlap of the π systems may be the reason why no topotactic single-crystal-to-single-crystal transformation is observed,^[36] unlike in the case of the parent acridizinium bromide (**1a**).^[14,15]

It might be tempting to assume that the photoreaction of naphthoquinolizinium **3a**(MeOH), crystallized from methanol, exhibited a remarkably low degree of conversion because photodimerization was taking place only at defect sites^[37–39] or on the surface^[40] of the crystal. Detailed inspection of the arrangement of this compound in the solid state, however, shows that pairs of molecules in the crystal lattice do indeed have a *limited* opportunity to dimerize in the crystalline phase (Figure 7). The structural parameters indicate that the arrangement is not ideal for solid-state photodimerization ($d = d' = 463$ pm), but that the π systems are close enough (ca. 360 pm) to provide topochemical excimer formation on irradiation.^[16,41] Such solid-state excimer formation may be detected by emission spectroscopy; both naphthoquinolizinium derivatives **3a** and **3b** exhibited solid-state emissions (see Figure 2 for **3a**), each with one broad band between 400 and 450 nm, apparently resulting from the monomer emission. Moreover, a significantly stronger emission band appeared, red-shifted compared to the fluorescence maximum in solution ($\Delta\lambda_{\text{em}} \approx 50$ nm), indicating excimer formation in the solid state.^[41] It may be conjectured that the molecules in this intermediate excimer could shift towards each other due to attractive interactions between the excited and ground-state molecules, such that a favourable arrangement for the photodimerization could be achieved. Such *non-topochemical* solid-state photoreactions are known, and are believed to proceed within a reaction cavity that provides enough freedom of movement.^[34]

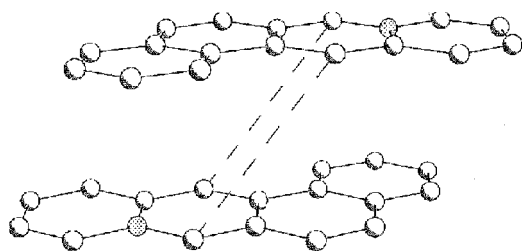


Figure 7. Arrangement of two molecules of **3a**(MeOH), crystallized from methanol, in the solid state (a pair of the two closest molecules is shown; counter-anions and lattice solvent are omitted for clarity, dotted lines indicate the bonds formed in the course of the photoreaction)

This assumption of initial excimer formation during the solid-state photodimerization was supported by the observation that irradiation of a solid sample of quinolizinium salt **3a**(EtOH) with monochromatic fluorescence spectrometer light ($\lambda = 380$ nm) resulted only in a decrease in the excimer emission intensity, whereas the monomer fluorescence remained unchanged (Figure 8).

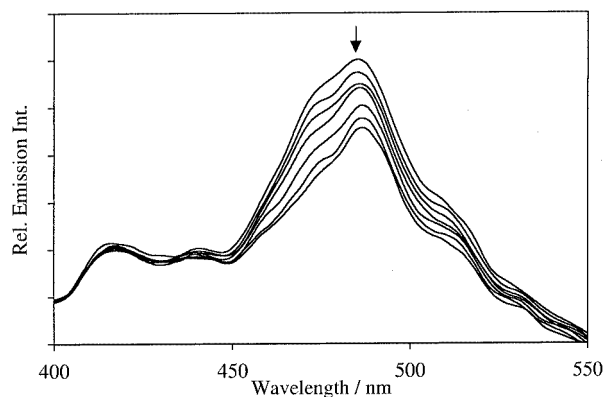


Figure 8. Solid-state emission spectra of **3a**(EtOH) upon irradiation ($\lambda = 380$ nm) of a crystalline sample for 6 h (the arrow indicates the successive decrease of the signal intensity on irradiation for 0, 1, 2, 3, 4, 5, and 6 h)

At the current stage, all explanations for the low degrees of conversion of some crystal modifications of **3a** and **3b** are speculative. Nevertheless, on the basis of the results obtained from **3a**(MeOH) we may reasonably infer that, at least in this case, the low level of conversion is the result of the arrangement of molecules in the bulk crystal, which provides some limited opportunities for solid-state photodimerization. However, it cannot be ruled out that a reaction cavity of appropriate size could be provided by defect sites within the crystalline sample.

It is interesting to note that the introduction of a benzene ring onto the acridizinium molecule did not result in arrangements of molecule pairs in the solid state different from those found in the parent acridizinium.^[14,16] If one assumes that a pair of molecules tends to achieve a maximum overlap of π systems,^[42] a *syn*-head-to-head arrangement of two molecules, and hence a photodimerization to the dimers *syn-hh-4a* and *syn-hh-4b*, should have been observed. Apparently, such an arrangement is energetically disfavoured due to repulsive ionic interactions, because the regions of molecules of equal polarity would be directly superimposed. Thus, in the absence of other intermolecular forces, the positive charge of the acridizinium cation has more influence than the π stacking on the arrangement of the two molecules. It may be noted that, in contrast to observations with the parent system,^[14] single-crystal quality was not required in the solid samples for regioselective photodimerization. Therefore, the annellation of another benzene moiety has presumably resulted in a stronger attractive interaction in the solid-state arrangement of acridizinium derivatives.

Experimental Section

General Remarks: ^1H and ^{13}C NMR: Bruker AC 200 (^1H : 200 MHz; ^{13}C : 50.3 MHz); Bruker DMX 600 (ROESY ^1H NMR: 600 MHz). ^1H NMR chemical shifts refer to $\delta_{\text{TMS}} = 0.0$ ppm; ^{13}C NMR chemical shifts refer to solvent signals ($[\text{D}_6]\text{DMSO}$: $\delta = 39.5$

ppm). Elemental analyses were performed at the Institute of Inorganic Chemistry, University of Würzburg. Melting points were determined with a Büchi B-545 and are uncorrected.

Absorption and Emission Spectra: UV/Vis: Hitachi U3200; emission: Perkin–Elmer LS50. Absorption and emission spectra were recorded in deoxygenated spectral-grade solvents (Fluka). Distilled water was further deionized by use of Millipore MilliQ equipment. If not noted otherwise, the solution concentrations were 10^{-4} M for absorption spectroscopy and 10^{-5} M for fluorescence spectroscopy. Emission spectra were recorded with an excitation wavelength close to the absorption maximum ($\lambda = 370$ and 380 nm). The relative fluorescence quantum yields were determined by the standard methodology^[43] with quinine sulfate in 1 N H_2SO_4 as reference ($\Phi_{\text{FI}} = 0.546$ ^[44]).

Irradiation in Solution and in the Solid State: Photoreactions were carried out with a 150-W high-pressure mercury lamp (Heraeus TQ 150, placed in a Duran glass cooling jacket) with a glass filter (Schott GG 395, $\lambda > 395$ nm). Samples were placed ca. 5 cm in front of the lamp. Irradiation with monochromatic light was performed with a spectrofluorimeter at room temperature (Perkin–Elmer LS 50, $\lambda = 380$ or 390 nm, excitation slit: 10.0 or 15.0). The solution photolyses were performed in methanol [$c(\mathbf{3a}) = 48$ mM; $c(\mathbf{3b}) = 50$ mM] at 10°C , and the photolysate was analysed after particular time intervals by ^1H NMR spectroscopy. Argon was bubbled through the methanol solutions for at least 10 min prior to irradiation, to provide oxygen-free solutions. The mass balance and the conversion was determined relative to dimethyl isophthalate or hexamethyldisiloxane as internal standards. The results are summarized in Table 2. Solid-state irradiation was carried out at 10°C with several solid samples, crystallized from different solvents. The ground solid was distributed on the inner walls of an NMR tube, and the photolysate was analyzed by ^1H NMR spectroscopy. The results are presented in Table 2. In preparative runs the solid samples were placed in the reaction vessel and flushed with argon. During irradiation the flask was frequently removed and placed in an ultrasonic bath for 1–2 min. Analysis of the reaction mixture by ^1H NMR showed the exclusive formation of the dimers **anti-ht-4** without any by-product.

anti-Head-to-Tail Photodimer of Naphtho[1,2-*b*]quinolizinium Bromide (3a): Naphtho[1,2-*b*]quinolizinium bromide (**3a**) was crystallized from ethanol. The ground crystals (14.3 mg, $43.6\ \mu\text{mol}$) were irradiated under argon for 60 h at 10°C . The resulting pale yellow solid was crystallized from methanol to give the dimer **anti-ht-4a** (7.40 mg, $11.2\ \mu\text{mol}$, 51%) as pale yellow cubes; m.p. $304\text{--}306^\circ\text{C}$ [dec., at $240\text{--}250^\circ\text{C}$, thermal cycloreversion was indicated by a colour change from pale yellow to green; m.p.(**3a**): $302\text{--}303^\circ\text{C}$]. UV (MeOH): λ (log ϵ) = 215 (4.78), 230 (4.91), 233 (4.93), 272 (4.18), 281 (b sh, 4.14), 314 (b sh, 3.65), 326 (b sh, 3.49) nm. ^1H NMR (600 MHz, $[\text{D}_6]\text{DMSO}$): δ = 7.17 (d, $J = 10.7$ Hz, 2 H, 13-H), 7.51–7.54 (m, 4 H, 7-H, 10-H), 7.63 (d, $J = 8.4$ Hz, 2 H, 6-H), 7.66 (ddd, $J = 8.0$, 6.8 Hz, 1.1 Hz, 2 H, 3-H), 7.83 (ddd, $J = 8.2$, 6.8 Hz, 1.3 Hz, 2 H, 2-H) 7.93 (d, $J = 8.2$ Hz, 2 H, 5-H) 7.96 (d, $J = 8.1$, 2 H, 4-H), 8.25–8.32 (m, 4 H, 12-H, 11-H), 8.52 (d, $J = 8.3$ Hz, 2 H, 1-H), 9.00 (d, $J = 5.9$ Hz, 2 H, 9-H) ppm. ^{13}C NMR (50 MHz, $[\text{D}_6]\text{DMSO}$): δ = 46.0 (C-13), 71.6 (C-7), 123.5 (C-1), 124.6 (C-6), 126.5 (C-10), 128.3 (C-3), 129.0 (C-2), 129.3 (C-12), 129.6 (C-4), 130.0 (C-13b), 130.3 (C-5), 130.4 (C-13a), 133.3 (C-4a), 134.7 (C-6a), 145.6 (C-9), 147.6 (C-11), 154.3 (C-12a). $\text{C}_{34}\text{H}_{24}\text{Br}_2\text{N}_2 + 2\text{H}_2\text{O}$ (656.4): calcd. C 62.21, H 4.30, N 4.27; found C 61.97, H 4.28, N 4.26.

anti-Head-to-Tail Photodimer of Naphtho[2,1-*b*]quinolizinium Bromide (3b): Naphtho[2,1-*b*]quinolizinium bromide (**3b**) was crystallized from methanol. The ground crystals (22.7 mg, $69.2\ \mu\text{mol}$) were irradiated under argon for 48 h at 10°C . The resulting pale yellow solid was crystallized from methanol to give the dimer **anti-ht-4b** (13.2 mg, $20.1\ \mu\text{mol}$, 58%) as pale yellow cubes; m.p. $310\text{--}311^\circ\text{C}$ [dec., at ca. $240\text{--}250^\circ\text{C}$, thermal cycloreversion was indicated by a colour change from pale yellow to green; m.p.(**3b**): $308\text{--}309^\circ\text{C}$]. UV (MeOH): λ (log ϵ) = 231 (4.91), 262 (b sh, 4.28), 275 (b sh, 4.20), 275 (b sh, 3.28) nm. ^1H NMR (600 MHz, $[\text{D}_6]\text{DMSO}$): δ = 6.53 (d, $J = 10.9$ Hz, 2 H, 7-H), 7.61 (d, $J = 8.3$ Hz, 2 H, 6-H), 7.65 (ddd, $J = 8.0$, 6.8 Hz, 1.0 Hz, 2 H, 3-H), 7.78 (ddd, $J = 7.7$, 6.0 Hz, 1.5 Hz, 2 H, 10-H), 7.85 (ddd, $J = 8.2$, 6.8 Hz, 1.3 Hz, 2 H, 2-H) 7.91 (d, $J = 8.1$ Hz, 2 H, 5-H), 7.93 (dd, $J = 8.1$, 1.2 Hz, 2 H, 8-H), 7.95 (d, $J = 8.1$ Hz, 2 H, 4-H), 8.08–8.12 (m, 4 H, 13-H and 9-H), 8.43 (d, $J = 8.3$ Hz, 2 H, 1-H), 9.37 (d, $J = 6.0$ Hz, 2 H, 11-H) ppm. ^{13}C NMR (50 MHz, $[\text{D}_6]\text{DMSO}$): δ = 51.0 (C-7), 69.1 (C-13), 124.4 (C-1), 126.6 (C-6), 127.8 (C-11), 128.8 (C-8), 129.0 (C-3), 129.9 (C-2), 130.2 (C-13b), 130.5 (C-4), 132.0 (C-5), 133.1 (C-6a), 133.5 (C-13a), 133.8 (C-4a), 145.8 (C-10), 146.3 (C-9), 153.1 (C-7a); $\text{C}_{34}\text{H}_{24}\text{Br}_2\text{N}_2 + 2\text{H}_2\text{O}$ (656.4): calcd. C 62.21, H 4.30, N 4.27; found C 62.41, H 4.38, N 4.25.

Irradiation of 3a(EtOH) in the Crystalline State, Monitored by Solid-State Emission Spectroscopy: A ground solid sample of **3a(EtOH)** was irradiated for 6 h at room temperature with the monochromatic light of a fluorescence spectrometer ($\lambda = 380$ nm, excitation slit: 15.0), and the reaction progress was monitored by emission spectroscopy (i.e., a solid-state fluorescence spectrum was recorded after every 30 min of irradiation). Figure 7 presents the spectra, with irradiation time intervals of 1 h. The position of the sample relative to the excitation light beam was not changed during the whole experiment.

Photoinduced Cycloreversion of anti-ht-4a and anti-ht-4b, Monitored by UV/Vis Spectroscopy: Solutions of the photodimers (**anti-ht-4a**: $5.0 \cdot 10^{-5}$ M; **anti-ht-4b**: $6.0 \cdot 10^{-5}$ M) in methanol (2 mL) were irradiated at room temperature with the monochromatic light of a fluorescence spectrometer ($\lambda = 390$ nm, excitation slit: 10.0), and the reaction progress was monitored by UV spectroscopy. Cycloreversion was indicated by the appearance of the characteristic $S_0\text{--}S_1$ absorption bands of the monomers **3a** and **3b**.

Photoinduced Cycloreversion of anti-ht-4b, Monitored by ^1H NMR Spectroscopy. a) A solution of the photodimer **anti-ht-4b** ($1.5 \cdot 10^{-2}$ M) in $[\text{D}_6]\text{DMSO}$ (0.5 mL) under argon was irradiated ($\lambda > 395$ nm) at room temperature, and the reaction progress was monitored by ^1H NMR spectroscopy. The photoinduced cycloreversion was indicated by the appearance of the characteristic ^1H NMR signals of the monomer **3b** (assigned by comparison with the ^1H NMR spectrum of an authentic sample). b) Compound **3b** (0.1 mol-equiv.) was added to a solution of the photodimer **anti-ht-4b** ($1.5 \cdot 10^{-2}$ M) in $[\text{D}_6]\text{DMSO}$ (0.5 mL). The solution was irradiated ($\lambda > 395$ nm) at room temperature, and the progress of the reaction was monitored by ^1H NMR spectroscopy. The results are shown in Figure 9.

Cycloreversions of anti-ht-4a and anti-ht-4b on Addition of Tris(bromophenyl)aminium Hexafluoroantimonate: An excess of tris(4-bromophenyl)aminium hexafluoroantimonate was added to a solution of **anti-ht-4b** ($6.0 \cdot 10^{-5}$ M) in DMF, and the reaction progress was monitored by UV spectroscopy. Directly after the addition, cycloreversion was indicated by the appearance of the characteristic $S_0\text{--}S_1$

Table 3. Crystallographic data of naphthoquinolinizinium bromides **3a(MeOH)** and **(3a(EtOH))**

	3a(MeOH) ^[a]	3a(EtOH) ^[b]
Empirical formula	C ₁₈ H ₁₆ BrNO	C ₁₈ H ₁₇ BrNO _{1.50}
Formula mass	342.23	351.24
Temperature [K]	193(2)	130(2)
Wavelength [Å]	0.71073	0.71073
Crystal system	monoclinic	triclinic
Space group	<i>P</i> 2 ₁ / <i>c</i>	<i>P</i> $\bar{1}$
<i>a</i> [Å]	7.6862(8)	7.2239(3)
<i>b</i> [Å]	7.9632(8)	9.8659(4)
<i>c</i> [Å]	24.559(3)	11.1942(4)
α [°]	90	72.8590(10)
β [°]	93.103(2)	80.6370(10)
γ [°]	90	89.1780(10)
Volume [Å ³]	1501.0(3)	751.74(5)
<i>Z</i>	4	2
Density (calculated) [Mg/m ³]	1.514	1.552
Absorption coefficient [mm ⁻¹]	2.737	2.737
<i>F</i> (000)	696	358
Crystal size [mm]	0.2 × 0.2 × 0.1	0.2 × 0.2 × 0.15
θ range for data collection [°]	1.66–26.08	2.16–26.01°
Index ranges	−9 ≤ <i>h</i> ≤ 9, 0 ≤ <i>k</i> ≤ 9, 0 ≤ <i>l</i> ≤ 30	−8 ≤ <i>h</i> ≤ 8, −11 ≤ <i>k</i> ≤ 12, 0 ≤ <i>l</i> ≤ 13
Reflections collected	23794	15372
Independent reflections	2975 [<i>R</i> (int) = 0.0296]	2939 [<i>R</i> (int) = 0.0231]
Completeness up to θ_{\max} (%)	99.9%	99.6%
Absorption correction	empirical	empirical
Refinement method	Full-matrix, least-squares on <i>F</i> ²	Full-matrix, least-squares on <i>F</i> ²
Data/restraints/parameters	2975/0/254	2939/4/217
Goodness-of-fit on <i>F</i> ²	1.023	1.081
Final <i>R</i> indices ^[c] ^[d] [<i>I</i> > 2 σ (<i>I</i>)]	<i>R</i> 1 = 0.0243; <i>wR</i> 2 = 0.0654	<i>R</i> 1 = 0.0255; <i>wR</i> 2 = 0.0661
<i>R</i> indices (all data)	<i>R</i> 1 = 0.0284; <i>wR</i> 2 = 0.0678	<i>R</i> 1 = 0.0280; <i>wR</i> 2 = 0.0676
<i>g</i> ₁ ; <i>g</i> ₂ ^[e]	0.0449, 0.3449	0.0427, 0.2891
Largest diff. peak/hole [e [−] Å ^{−3}]	0.367/−0.287	0.661/−0.245

[a] Contains methanol. [b] Contains ethanol and water. [c] $R1 = \sum ||F_o| - |F_c|| / \sum |F_o|$. [d] $wR2 = [\sum w(F_o^2 - F_c^2)^2 / \sum w(F_o^2)^2]^{0.5}$. [e] $w = [\sigma^2(F_o^2) + (g_1P)^2 + g_2P]^{-1}$, $P = 1/3[\max(F_o^2, 0) + 2F_c^2]$.

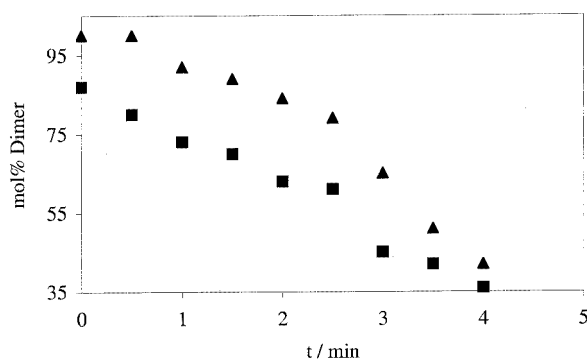


Figure 9. Photoinduced cycloreversion of the dimer **anti-ht-4b**, monitored by ¹H NMR spectroscopy [λ > 395 nm, *c*(**anti-ht-4b**) = $1.5 \cdot 10^{-2}$ M, ▲: no **3b** added; ■: 0.1 mol-equiv. of **3b** added]

absorption band (maximum with lowest wavelength: λ = 393 nm) of the monomer **3b**.

Crystal Data for 3a(MeOH) (Crystallized from Methanol) and 3a(EtOH) (Crystallized from Ethanol): The data from shock-cooled

crystals were collected with a Bruker SMART-APEX diffractometer with D8 goniometer (graphite-monochromated Mo-*K*_α radiation, λ = 0.71073 Å) equipped with a low-temperature device in ω -scan mode at 193(2) K [**3a(MeOH)**] and 130(2) K [**3a(EtOH)**].^[45] The data were integrated with SAINT^[46] and an empirical absorption correction was applied.^[47] The structures were solved by direct methods (SHELXS-97)^[48] and refined by full-matrix, least-squares methods against *F*² (SHELXL-97).^[49] All non-hydrogen atoms were refined with anisotropic displacement parameters. All hydrogen atoms in **3a(MeOH)** were located by difference Fourier syntheses and refined without any distance or thermal motion constraints. In **3a(EtOH)** all hydrogen atoms bonded to sp²-carbon atoms were assigned ideal positions and refined with a riding model, with *U*_{iso} constrained to 1.2 times the *U*_{eq} value of the parent atom. The hydrogen atoms of the solvent molecules were located by difference Fourier synthesis and refined by use of distance restraints and thermal motion constraints as for **3a** (Table 3). CCDC-171967 and -171968 contain the supplementary crystallographic data for this paper. These data can be obtained free of charge at www.ccdc.cam.ac.uk/conts/retrieving.html or from the Cambridge Crystallographic Data Centre, 12, Union Road, Cambridge CB2 1EZ, UK [Fax: (internat.) + 44-1223/336-033; E-mail: deposit@ccdc.cam.ac.uk].

Acknowledgments

This work was generously financed by the Deutscher Akademischer Austauschdienst (VIGONI program), the Deutsche Forschungsgemeinschaft and the Fonds der Chemischen Industrie. Constant encouragement and generous support by Prof. W. Adam is gratefully appreciated. We would like to thank Dr. M. Grüne and Mrs. E. Ruckdeschel for the recording of ROESY NMR spectra and the referees for some helpful comments.

- [1] *Photochemistry in Organized and Constrained Media* (Ed.: V. Ramamurthy), VCH-Publishers, New York, **1991**.
- [2] *Reactivity in Molecular Crystals* (Ed.: Y. Ohashi), VCH-Publishers, New York, **1994**.
- [3] M. Sakamoto, *Chem. Eur. J.* **1997**, *3*, 684–689.
- [4] H. Ihmels, J. R. Scheffer, *Tetrahedron* **1999**, *55*, 885–907.
- [5] Y. Ito, *Synthesis* **1998**, 1–32.
- [6] G. M. J. Schmidt, *Pure Appl. Chem.* **1971**, *27*, 647.
- [7] M. D. Cohen, B. S. Green, *Chem. Br.* **1973**, *9*, 490.
- [8] S. McN. Sieburth, *Adv. Cycloadd.* **1999**, *5*, 85–118.
- [9] S. McN. Sieburth, N. T. Cunard, *Tetrahedron* **1996**, *52*, 6251–6282.
- [10] G. Kaupp, *Angew. Chem.* **1992**, *104*, 435–437; *Angew. Chem. Int. Ed. Engl.* **1992**, *31*, 422.
- [11] C. K. Bradsher, in: *Comprehensive Heterocyclic Chemistry* (Eds.: A. J. Boulter, A. McKillop) Oxford, Pergamon Press, **1985**, vol. 2, p. 525.
- [12] H. Bouas-Laurent, A. Castellán, J.-P. Desvergne, R. Lapouyade, *Chem. Soc. Rev.* **2000**, *29*, 43–55.
- [13] H. Bouas-Laurent, J.-P. Desvergne, in: *Photochromism, Molecules and Systems* (Eds.: H. Dürr, H. Bouas-Laurent), Elsevier, Amsterdam, **1990**, chapter 14.
- [14] W. N. Wang, W. Jones, *Tetrahedron* **1987**, *43*, 1273–1279.
- [15] W. N. Wang, W. Jones, *Mol. Cryst. Liq. Cryst.* **1994**, *242*, 227–240.
- [16] D. K. Kearsley, in: *Organic Solid State Chemistry* (Ed.: G. R. Desiraju), Elsevier, Amsterdam, **1987**, chapter 3.
- [17] C. Lehnberger, D. Scheller, T. Wolff, *Heterocycles* **1997**, *45*, 2033–2039.
- [18] H. Ihmels, D. Leusser, M. Pfeiffer, D. Stalke, *Mol. Cryst. Liq. Cryst.* **2001**, *356*, 433–441.
- [19] H. Ihmels, D. Leusser, M. Pfeiffer, D. Stalke, *J. Org. Chem.* **1999**, *64*, 5715–5718.
- [20] J. P. Glusker, *Top. Curr. Chem.* **1998**, *198*, 1.
- [21] A. Nangia, G. R. Desiraju, *Top. Curr. Chem.* **1998**, *198*, 57.
- [22] G. Kaupp, H. Frey, G. Behmann, *Chem. Ber.* **1988**, *121*, 2135.
- [23] J. Vansant, S. Toppet, G. Smets, J. P. Declercq, G. Germain, M. Van Meersche, *J. Org. Chem.* **1998**, *45*, 1565.
- [24] C. K. Bradsher, L. E. Beavers, *J. Am. Chem. Soc.* **1956**, *78*, 2495–2462.
- [25] One of the referees has pointed out that it is misleading to use formulas **3a** and **3b** for the different crystal modifications obtained by crystallization from different solvents. Thus, the different solid samples are indexed by the corresponding solvent in brackets.
- [26] A. Schönberg, A. Mustafa, M. Z. Barakat, N. Latif, R. Moubasher, A. Mustafa, *J. Chem. Soc.* **1948**, 2126–2129.
- [27] S. Singh, C. Sandorfy, *Can. J. Chem.* **1969**, *47*, 259–263.
- [28] For photocycloadditions of benzo[*a*]anthracene to anthracene derivatives see: R. Lapoyade, A. Castellán, H. Bouas-Laurent, *Tetrahedron Lett.* **1969**, 3537–3540.
- [29] Although, Wolff et al. reported a hh:ht ratio of ca. 85:10 of dimers **2a** on irradiation of **1a** in water (ref.^[17]), we observed a ratio of 51:49 on photolysis in methanol (determined by ¹H NMR spectroscopic analysis; conversion: 34%, product balance 34%, $\lambda = 385$ nm).
- [30] R. A. Barber, P. de Mayo, K. Okada, S. K. Wong, *J. Am. Chem. Soc.* **1982**, *104*, 4995–4996.
- [31] J. M. Masnovi, J. K. Kochi, *J. Am. Chem. Soc.* **1985**, *107*, 6781.
- [32] The cycloreversion of the photodimers **2a** by photoinduced electron transfer in the presence of erythrosine has also been observed: R. Mitzner, J. Bendig, D. Kreysig, *Z. Chem.* **1986**, *26*, 255–256.
- [33] R. Mitzner, J. Bendig, R. Ziebig, F. Graichen, D. Kreysig, F. Pragst, *J. Prakt. Chem.* **1985**, *327*, 241–250. The reported reduction potential was determined vs. SCE in 0.1 M TEAP/DMF. This potential was adjusted to that relative to NHE (–0.67 V). The reduction potential in the excited state was estimated by $E^*_{\text{Red}} = E^0_{\text{Red}} + E_{0,0}$, with $E_{0,0} = 3.10$ eV.
- [34] V. Ramamurthy, in: *Photochemistry in Organized and Constrained Media* (Ed.: V. Ramamurthy), VCH-Publishers, New York, **1991**, chapter 4.
- [35] C. Hunter, *Chem. Soc. Rev.* **1994**, 101.
- [36] For an almost complete compilation of single-crystal-to-single-crystal photoreactions, see ref.[30] in: M. Leibovitch, G. Olovson, J. R. Scheffer, J. Trotter, *J. Am. Chem. Soc.* **1998**, *120*, 12755.
- [37] D. P. Craig, P. Sarti-Fantoni, *J. Chem. Soc., Chem. Commun.* **1966**, 742.
- [38] M. D. Cohen, Z. Ludmer, J. M. Thomas, J. O. Williams, *J. Chem. Soc., Chem. Commun.* **1969**, 1172.
- [39] J. M. Thomas, S. Morsi, J.-P. Desvergne, *Adv. Phys. Org. Chem.* **1977**, *15*, 63.
- [40] G. Kaupp, *Angew. Chem.* **1992**, *104*, 609–612; *Angew. Chem. Int. Ed. Engl.* **1992**, *31*, 595.
- [41] Y. Yakot, M. D. Cohen, Z. Ludmer, *Adv. Photochem.* **1979**, *11*, 489–523.
- [42] The extension of the π surface by one benzene moiety, for example, increases the binding energy in a π -stacked arrangement by about 0.4 kcal/mol: J. Rebek, *Angew. Chem. Int. Ed. Engl.* **1990**, *29*, 245.
- [43] J. N. Demas, G. A. Crosby, *J. Phys. Chem.* **1971**, *75*, 991–1024.
- [44] D. F. Eaton, *Pure Appl. Chem.* **1988**, *60*, 1108–1114.
- [45] D. Stalke, *Chem. Soc. Rev.* **1998**, *27*, 171–178.
- [46] Bruker-Nonius Inc., *SAINT-NT*, Madison, WI, **2000**.
- [47] G. M. Sheldrick, *SADABS 2.0*, University of Göttingen, **2000**.
- [48] G. M. Sheldrick, *Acta Crystallogr., Sect. A* **1990**, *46*, 467–473.
- [49] G. M. Sheldrick, *SHELXL-97*, University of Göttingen, **1997**.

Received October 18, 2001

[O01499]